A&A 531, A139 (2011)
DOI: 10.1051/0004-6361/201015374

Astronomy & Astrophysics

Network velocity gradients in the photosphere

I. Modeling

G. Molodij, V. Bommier, and J. Rayrole*

Observatoire de Paris-Meudon, LESIA, 5 place J. Janssen, 92195 Meudon principal, UMR 8109 CNRS, France
e-mail: guillaume.molodij@obspm.fr

Received 10 July 2010 / Accepted 9 May 2011

ABSTRACT

We present an extension of the Unno-Rachkovsky solution that provides the theoretical profiles coming out of a Milne-Eddington atmosphere imbedded in a magnetic field, and that then takes a vertical velocity gradient into account. Thus, the theoretical profiles may display asymmetries as do the observed profiles, which facilitates the inversion based on the Unno-Rachkovsky theory, and leads to the additional determination of the vertical velocity gradient. We present UNNOFIT inversion on synthetic data and spectropolarimetric observations performed on an active region of the Sun with the French-Italian telescope THEMIS operated by CNRS and CNR on the island of Tenerife.

Key words. Sun: photosphere – line: profiles – magnetic fields – instrumentation: polarimeters

1. Introduction

The first interpretations of line asymmetries (ignoring polarization) in terms of convective inhomogeneities of the solar photosphere were published by Voigt (1957) and Schröter (1958). This asymmetry (the so-called C-shape) is a sensitive measure of the hydrodynamic structure of the photospheric layers and is caused by the spatially and temporally averaged convective motions of the solar atmosphere (Kaisig & Schröter 1983). The line is also sensitive to atmospheric fields quantities like the bulk velocity (Grossmann-Doerth 1994). Gradients in thermodynamic parameters and line-of-sight velocity may produce quite dissymmetric line profiles, so that one might infer the differential bulk motion (i.e., line of sight average Doppler velocity) in a quantitative form (Lites et al. 1990).

Many observations of solar Stokes profiles show asymmetries that can be explained by depth gradients in the line-of-sight velocity (Auer & Heasley 1978; Landolfi & Landi Degl'Innocenti 1996). Fourier transform spectrometer (FTS) observations at disk center (Stenflo et al. 1984) have shown that Stokes V profiles have larger blue lobes than red ones, indicating the presence of such gradients, if we exclude other explanations related to non-LTE effects (Solanki 1986; Pantellini et al. 1988). Observations of asymmetries with good spatial resolution have been published by Grossmann-Doerth (Grossmann-Doerth 1996), and observations taken with the Advanced Stokes Polarimeter (ASP) by Martinez-Pillet et al. (1997) show also evidence of asymmetries in Stokes Q and U. Sanchéz Almeida & Lites (1992) show that the observations can be reproduced by postulating sufficiently large vertical velocity gradients. More recently, the results of Auer & Heasley have been extended by López Ariste (2002) to a more general case including anomalous dispersion to conclude that velocity gradients are a sufficient condition for the presence of asymmetries.

We present a model involving a flow inside a magnetic element with a gradient along the line of sight to reproduce the observed asymmetry that has been implemented in our inversion code. This UNNOFIT inversion code is based on the Marquardt algorithm to reach the minimum theory/observation discrepancy with the theoretical profiles given by the Unno Rachkovsky solution. Pionereed by Harvey et al. (1972) and Auer et al. (1977), this technique has been improved by Landolfi & Landi Degl'Innocenti (1982) and Landolfi et al. (1982) to allow for magneto-optical and damping effects. The same Marquardt algorithm technique, based on the Unno Rachkovsky solution that includes the magneto-optical effects as introduced by Landolfi & Landi Degl'Innocenti (1982) has been applied to sunspot-observation inversion by Skumanich & Lites (1987) and Lites & Skumanich (1990), who implemented additional reduction procedures in their code. Bommier et al. (2007) complemented the UNNOFIT code by introducing a two-component atmosphere, having a magnetic and a nonmagnetic component. One of the great advantages of the UNNOFIT method is to use analytical profiles and the Marquardt algorithm to fit the observed profiles. Inversion techniques developed by Skumanich & Lites (1987) are used to process SOT/HINODE data, as well as SIR code based on response functions developed by Del Toro Iniesta & Ruiz Cobo (1996).

The plan of the paper is as follows. We present in Sect. 2 the modified Unno theory for velocity gradients and examples of modeling on line profiles in Sect. 3. UNNOFIT inversions are tested in Sect. 4 on synthetic data. Results of spectropolarimetric observations performed on an active region of the Sun with the French-Italian telescope THEMIS operated by the CNRS and CNR on the island of Tenerife are presented in Sect. 5.

2. The Unno theory modified for velocity gradients

The line formation in the presence of a magnetic field has been studied by several authors, but especially by Unno (1956),

* In memory of our friend and colleague Jean Rayrole.

Stepanov (1961) and Rachkovsky (1961). A straightforward calculation by Landi Degl'Innocenti (2004) yields the expressions of the Unno-Rachkovsky solutions, including magneto-optical effects,

$$\begin{aligned}
I(0,\mu) &= B_0\left\{1+\beta\mu\Delta^{-1}(1+k_I)\left[(1+k_I)^2\right.\right.\\
&\quad \left.\left.+f_Q^2+f_U^2+f_V^2\right]\right\}\\
Q(0,\mu) &= -B_0\beta\mu\Delta^{-1}\Big\{(1+k_I)^2k_Q-(1+k_I)\\
&\quad \times(k_Uf_V-k_Vf_U)+f_Q(k_Qf_Q+k_Uf_U+k_Vf_V)\Big\}\\
U(0,\mu) &= -B_0\beta\mu\Delta^{-1}\Big\{(1+k_I)^2k_U-(1+k_I)\\
&\quad \times(k_Vf_Q-k_Qf_V)+f_U(k_Qf_Q+k_Uf_U+k_Vf_V)\Big\}\\
V(0,\mu) &= -B_0\beta\mu\Delta^{-1}\Big\{(1+k_I)^2k_V-(1+k_I)\\
&\quad \times(k_Qf_U-k_Uf_Q)+f_V(k_Qf_Q+k_Uf_U+k_Vf_V)\Big\}
\end{aligned} \tag{1}$$

where

$$\begin{aligned}
\Delta &= (1+k_I)^4+(1+k_I)^2\left(f_Q^2+f_U^2+f_V^2-k_Q^2-k_U^2-k_V^2\right)\\
&\quad -(k_Qf_Q+k_Uf_U+k_Vf_V)^2,
\end{aligned}$$

and where B_0 and β represent the surface value and the slope of the Planck function. Here, $\mu = \cos\alpha$, where α is the angle between the ray path and the direction outward along the vertical to the atmosphere. In the case of the local thermodynamical equilibrium (LTE),

$$\begin{aligned}
k_I &= K_{\rm L}h_I & f_Q &= K_{\rm L}r_Q\\
k_Q &= K_{\rm L}h_Q & f_U &= K_{\rm L}r_U\\
k_U &= K_{\rm L}h_U & f_V &= K_{\rm L}r_V\\
k_V &= K_{\rm L}h_V
\end{aligned} \tag{2}$$

where $K_{\rm L} = k_{\rm L}/(\Delta\nu_{\rm D}k_{\rm c})$ is the ratio between the frequency integrated line absorption coefficient and the continuum absorption coefficient at the line wavelength, and $\Delta\nu_{\rm D}$ is the Doppler width ($K_{\rm L}$ is expressed in Doppler width units). The ratio between the line absorption coefficient at line center and the continuum absorption coefficient is η_0,

$$\begin{aligned}
h_I &= \frac{1}{2}\left[\eta_p\sin^2\theta+\frac{\eta_b+\eta_r}{2}\left(1+\cos^2\theta\right)\right]\\
h_Q &= \frac{1}{2}\left[\eta_p-\frac{\eta_b+\eta_r}{2}\right]\sin^2\theta\cos 2\chi\\
h_U &= \frac{1}{2}\left[\eta_p-\frac{\eta_b+\eta_r}{2}\right]\sin^2\theta\sin 2\chi\\
h_V &= \frac{1}{2}\left[\eta_r-\eta_b\right]\cos\theta\\
r_Q &= \frac{1}{2}\left[\rho_p-\frac{\rho_b+\rho_r}{2}\right]\sin^2\theta\cos 2\chi\\
r_U &= \frac{1}{2}\left[\rho_p-\frac{\rho_b+\rho_r}{2}\right]\sin^2\theta\sin 2\chi\\
r_V &= \frac{1}{2}\left[\rho_r-\rho_b\right]\cos\theta
\end{aligned} \tag{3}$$

for zero magnetic field and no damping by $K_{\rm L}/\sqrt{\pi}$, where $\eta_{p,b,r}$ and $\rho_{p,b,r}$ denote the Zeeman component absorption and dispersion profile, respectively. They are normalized to unity in reduced frequency $v = \nu/\Delta\nu_{\rm D}$. Index p refers to the transition for which the change in the magnetic quantum number is $\Delta m = 0$ (π oscillator in the Lorentz theory). For b and r, $\Delta m \pm 1$, we have the $\sigma_\pm$ components. Equation (1) provides simple analytical expressions of the Stokes parameters profiles of the line radiation emerging from a magnetized stellar atmosphere, although the Milne-Eddington model is the simplest schematization of a stellar atmosphere. By setting $f_Q = f_U = f_V = 0$, one obtains the simplified Unno solutions. The dependence on the parameter B_0 of the Planck function is dropped by normalizing the profiles to the intensity $I_{\rm c}(0,\mu)$ of the nearby continuum.

We present modeling that involves a flow inside a magnetic element with a gradient along the line of sight to reproduce the observed asymmetry. The comparison between the modeling and observations leads us to call in question again the hypothesis of a stationary flow inside the magnetic element. The first reason is that the stationary flow does not describe the behavior of the mean slope bisector that is proportional to the velocity gradients. Second, both Ribes et al. (1985) and Solanki & Pahkle (1988) show that the calculated profiles completely fail to match the observations, especially in the comparison of lines with different stengths and excitation potentials. A comparison between the modeling and observations leads us to allot a wavelength distribution function proportional to the profile itself to the velocity gradient in order to keep the linear behavior of the mean bisectors we observed. We modified the absorption coefficient entering the Unno-Rachkovsky formalism, Unno (1956), Rachkovsky (1961). To generalize the transfer equations to account for the magnetic field splitting in the presence of a velocity field gradient, we propose the following modification of the quantities $\eta_{p,b,r}$.

We let v_r be the radial velocity at the line center formation depth and v_h the Zeeman shift expressed both in Doppler width unit expressed by $\xi = \Delta\lambda_{\rm D}$ to match the different observed line profiles,

$$\begin{aligned}
v_r &= \alpha\,\frac{v_{\rm s}}{\xi}\\
v_h &= \frac{4,67\times10^{-2}\lambda^2\bar{g}H}{\xi}
\end{aligned} \tag{4}$$

where $v_{\rm s}$ is the velocity expressed in ms^{-1}, $\bar{g}$ is the effective Landé factor, and α a constant to convert the velocity in Doppler width unit (Angstroms). Introducing the velocity gradient denoted δ_V (the velocity is the difference between the line center and far wings formation depths), one obtains the absorption coefficients $\eta_{p,b,r}$, respectively, for each of the π, σ_+ and σ_- components,

$$\begin{aligned}
\eta_p &= \eta_0\ \exp\left[-\left(\frac{\lambda-\lambda_0}{\xi}+v_r+\delta V_p\right)^2\right]\\
\eta_b &= \eta_0\ \exp\left[-\left(\frac{\lambda-\lambda_0}{\xi}-v_h+v_r+\delta V_l\right)^2\right]\\
\eta_r &= \eta_0\ \exp\left[-\left(\frac{\lambda-\lambda_0}{\xi}+v_h+v_r+\delta V_r\right)^2\right]
\end{aligned} \tag{5}$$

with

$$\delta V_p = \frac{\delta_V}{\xi} \exp\left[-\left(\frac{\lambda-\lambda_0}{\xi}+v_r\right)^2\right]$$
$$\delta V_b = \frac{\delta_V}{\xi} \exp\left[-\left(\frac{\lambda-\lambda_0}{\xi}-v_h+v_r\right)^2\right]$$
$$\delta V_r = \frac{\delta_V}{\xi} \exp\left[-\left(\frac{\lambda-\lambda_0}{\xi}+v_h+v_r\right)^2\right]. \quad (6)$$

3. Modeling the velocity gradients

A question arises about the symmetrization of the polarized profiles that are broken, in particular, by the velocity effects. In our previous works, we used the line position determination method proposed by Bommier & Rayrole (2002). In previous analysis (Bommier et al. 2005), since Q and U are symmetrical profiles, all the $I+Q$, $I-Q$, $I+U$, and $I-U$ profiles are displaced in frequency by the radial velocity alone and not by the magnetic field. The correction consists then in recentering all the individual profiles $I+Q$, $I-Q$, $I+U$, and $I-U$ at each of the two times of the beam exchange before combining them for extracting Q/I and U/I. The situation is more complex with V, because $I+V$ and $I-V$ are displaced in frequency by both the radial velocity and the magnetic field. Figure 1 shows the behavior of the bisector position of $I+V$ and $I-V$ as a function of the wavelength assuming an homogenous atmosphere. A basic result is that the bisectors behave as a linear function of the wavelength, regardless of the magnetic field field and velocity gradient. With a zero velocity gradient, the $I+V$ and $I-V$ bisector slopes always have opposite signs and the bisectors are symmetrical with respect to the bisector position in the absence of a magnetic field. When a non-zero velocity gradient is introduced, all these bisectors bend in the same way, but keep their linear behavior, as is visible in Fig. 1 where we show an example for Fe I 6301.5 Å with parameters $\eta_0 = 0.8$, $\xi = 50$, $B = 1000$ G, $\psi = 60^o$ and a velocity gradient, $\delta_V = -800$ m s^{-1}. The resulting V Stokes profile is plotted in the bottom part of the figure and is asymmetric. We succeeded in reproducing the observed V asymmetry of a series of lines of different strengths and excitation potentials with the velocity gradient assumption. In contrast, we verified that the contribution of the variation in the thermodynamical parameters along the line of sight, suggested by Solanki & Pahkle (1988), cannot explain the observed asymmetries.

Figure 2 presents a modeling of the dissymmetries between $I+V$ and $I-V$ and the corresponding Stokes V asymmetry for increasing values of negative velocity gradients ($\delta_V = -300$, -800, and -1400 m s^{-1}). The $I+V$ and $I-V$ profiles are identical for $B = 0$ and $\delta_V = 0$. When B increases, the bisector positions shift almost linearly and symmetrically. This is the linear and symmetrical behavior that suggested the theoretical formalism introduced in Sect. 2. Figure 3 displays $I+V$ and $I-V$ dissymmetries and related Stokes V asymmetry for Fe I 5247.06 Å, Fe I 6151.6 Å, and Fe I 6302.5 Å with a velocity gradient of $\delta_V = -800$ m s^{-1}). Dissymmetry appears between the $I+V$ and $I-V$ positions and depends both on the sign of the gradient and on the sign of the magnetic polarity. In the presence of a magnetic field, the slope of the line defined by the bisector positions derived at different depths in the profiles of $I+V$ and $I-V$ increases or decreases, respectively, according to the sign of the velocity gradient. In the case of Figs. 2 and 3 involving a negative velocity gradient, $I-V$ bisector positions slope increases,

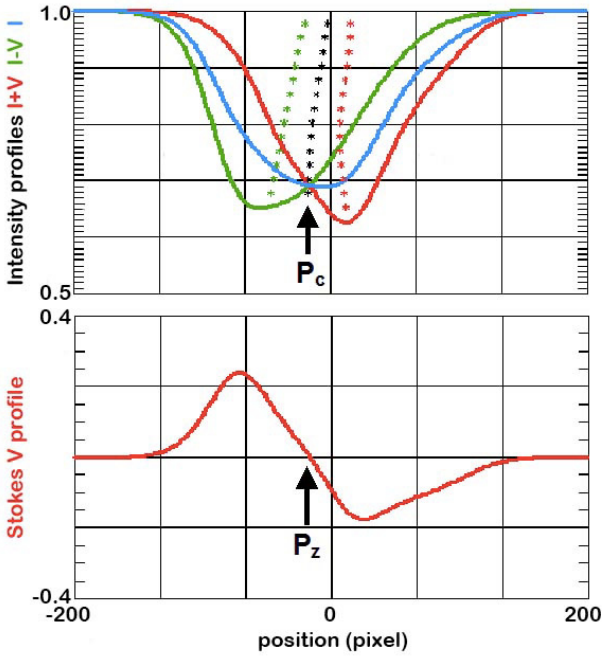

Fig. 1. *Top*: modeling of $I+V$ (red curve) and $I-V$ (green curve) for Fe I 6301.5 Å in the presence of a magnetic field and velocity gradient (here $\eta_0 = 0.8$, $\xi = 50$, $B = 1000$ G, $\psi = 60^o$, and $\delta v = -800$ m s^{-1}. The blue curve is for the I Stokes. The plotted stars define the bisector positions derived at different depths in the profiles, and the black stars represent the bisector half summation. P_c is the intersection point between $I+V$ and $I-V$ that is distinct from the I Stokes minimum. Bottom: modeling of the corresponding V Stokes. P_z is the position of the Stokes V zerocrossing.

while the $I+V$ one decreases linearly as a function of the velocity gradient. These ascertainments remain in the case of positive velocity gradients, by inverting the effects on $I-V$ and $I+V$. We notice that observed profiles are properly fitted when introducing the velocity gradient modeling that facilitates the inversion derivation. We have already introduced the modifications in our UNNOFIT inversion code in the Milne-Eddington assumption with success.

4. UNNOFIT inversion including velocity gradients

As described by its authors (Landolfi et al. 1982), UNNOFIT provides simultaneous determination of eight free parameters via the fit of the four Stokes profiles. The eight free parameters are 1) the line strength η_0; 2) the Zeeman splitting $\Delta\lambda_H$ that provides the magnetic field strength; 3) the Doppler absorption profile width $\Delta\lambda D$; 4) the γ damping parameter of the Voigt function; 5) one single b parameter describing the Milne Eddington τ dependence along the atmosphere vertical with $b = \mu B_1/B_0$, where B_0 and B_1 are the usual parameters describing the Milne Eddington atmosphere, and μ is the cosine of the line of sight inclination angle; 6) the line central wavelength (providing thus the Doppler shift); 7) and 8) are the magnetic field inclination and azimuth angles. Bommier et al. (2007) added a ninth free parameter, the filling factor α, which means that the received radiation is the sum of the magnetic component radiation, weighted α, and of the non-magnetic component one, weighted $1-\alpha$. The Marquardt algorithm is an iterative method of reaching the minimum of the chi-square parameter that characterizes the theory/observation discrepancy. It makes

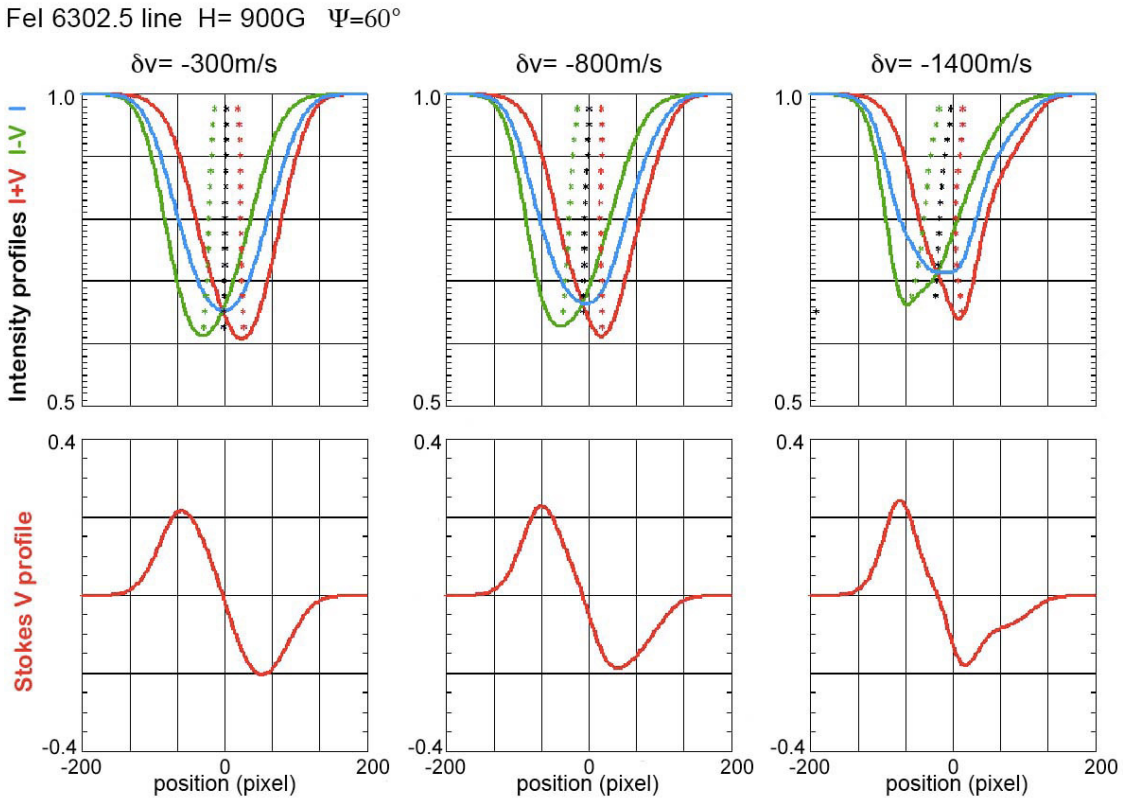

Fig. 2. Modeling of $I + V$ and $I - V$ dissymmetries and related Stokes V asymmetry for Fe I 6302.5 Å and three values of the velocity gradient ($\delta_V = -300$, -800, and -1400 m s^{-1}).

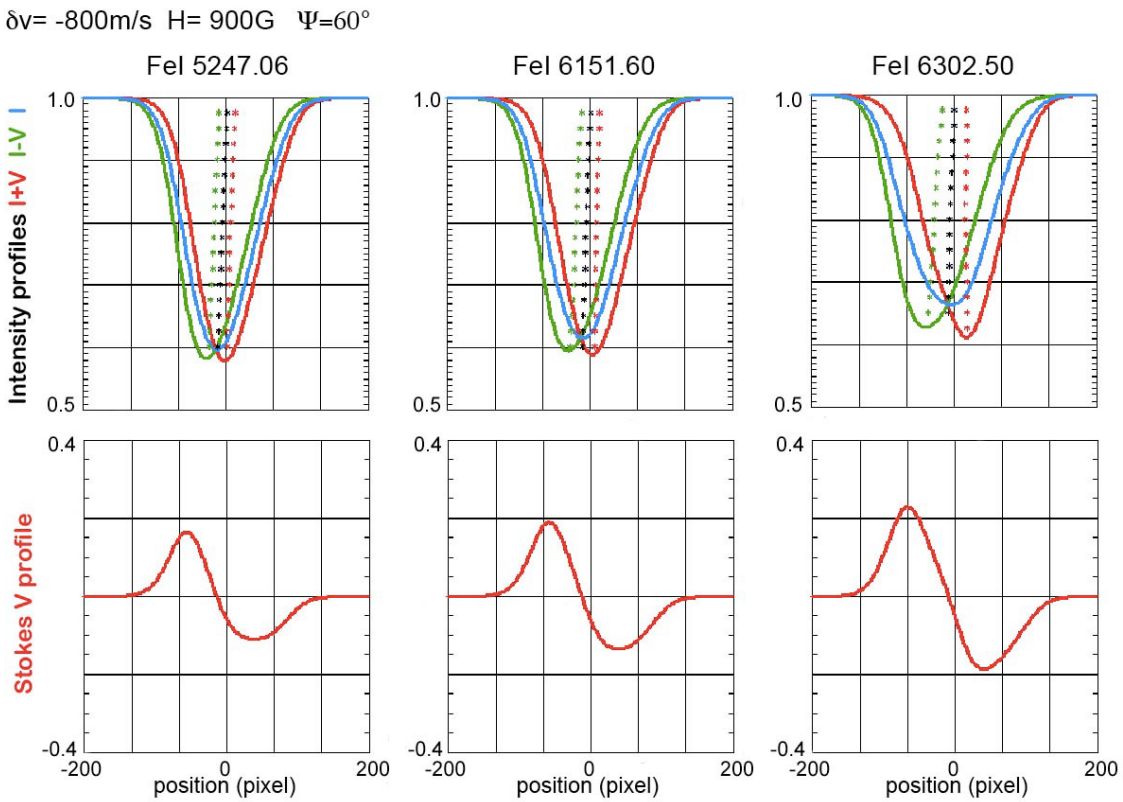

Fig. 3. Modeling of $I + V$ and $I - V$ dissymmetries and related Stokes V asymmetry for Fe I 5247.06 Å, Fe I 6151.6 Å , and Fe I 6302.5 Å with a velocity gradient of $\delta_V = -800$ m s^{-1}.

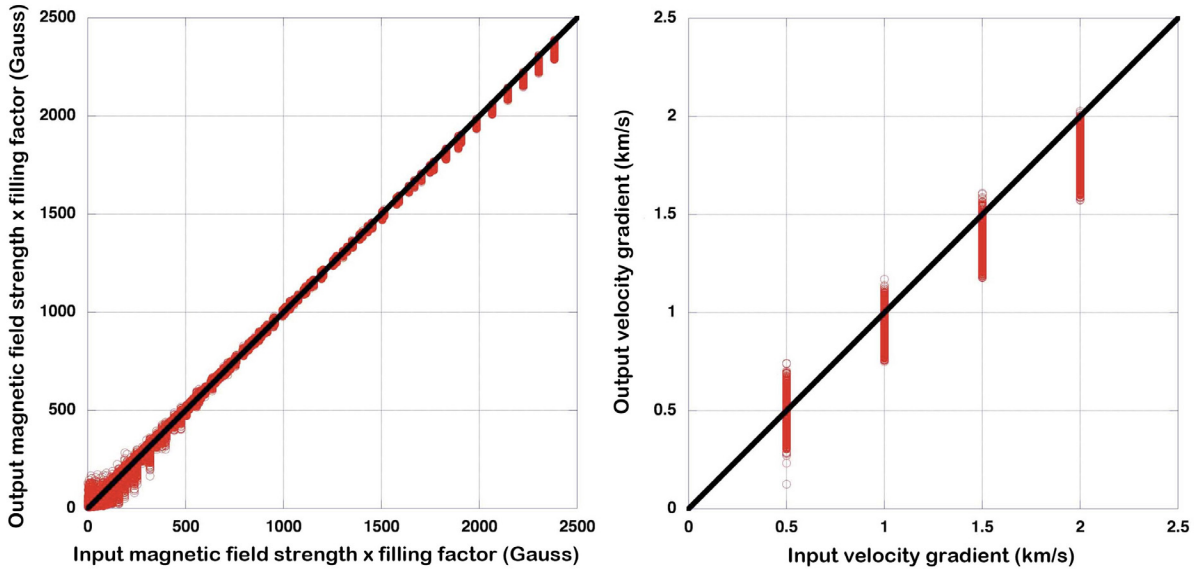

Fig. 4. Comparison between the UNNOFIT output values with the input ones of a series of synthetic profiles of the line CaI 6103. For each ensemble of input values (abscissae), a set of theoretical profiles has been computed, noised, and then inverted, leading to the output (ordinate). *Left*: the local velocity gradient. Å. *Right* the local average magnetic field strength, which is the product of the magnetic field strength by the magnetic filling factor.

use of the partial derivatives of the functions giving the observed parameters with respect to the parameters to be determined. With this purpose, these functions ought to be analytical functions so that their derivatives can be written down explicitly. This requirement is fulfilled by the Unno-Rachkovsky solution in the Milne Eddington atmosphere. The iteration is initialized by a random draw of the nine parameters. This random character has led to repeating the iteration for each pixel 20 times, with a different initial draw each time. The iteration is stopped when one of the three following requirements is fulfilled: a) when the number of iterations gets larger than a previously fixed number (presently 60); b) when the chi-square gets smaller than a small fraction (presently 10^{-10} of the initial chi-square (the one calculated at the beginning with random numbers); c) when the sum of the absolute values of the eight increments gets smaller than a fixed number. The final result is the one corresponding to the lowest chi-square value of the 20 iterations.

4.1. Inversion tests

To investigate the inversion accuracy, we proceeded in a pragmatic manner. Given (i) a series of 183 600 field (field strength ranging from 100 to 3000 Gauss with 100 Gauss steps; (ii) field inclination ranging from 10° to 170°; and (iii) azimuth ranging from 0° to 170°, both with 10° steps, 20 filling-factor values ranging in a logarithmic scale between 0.01 and <1), we computed the theoretical profiles that would result from these fields, by applying the Unno-Rachkowsky solution. We then added a noise to these theoretical profiles. The noise followed a uniform distribution (FORTRAN ran function), a random number taken between -3×10^{-3} and $+3 \times 10^{-3}$ (given the noise level 1.5×10^{-3} in the observed profiles). We submitted these noised theoretical profiles to the UNNOFIT inversion, and then compared the obtained magnetic fields (output) with the initial ones (input). The first result (Fig. 4) is that the local velocity gradient is determined. The simulated profiles are properly fitted when introducing the velocity gradients modeling so that the inversion derivation is facilitated. As already indicated in Bommier et al. (2007), although the magnetic field strength B and magnetic filling factor α are not separately recovered by the inversion, their product αB is. The value of αB is the local average magnetic field strength, and the magnetic flux is only the longitudinal component of the corresponding vector. As the present method only permits the determination of the local average field αB, we consider this quantity (together with the field direction) instead of α and B separately in the following. The histograms of the differences output minus input are displayed in Fig. 5. We put the histogram widths in the same category as the UNNOFIT accuracy under our observation conditions. Five Gauss can be considered as the magnetic field accuracy of the present measurements, and was also, in accordance, the accuracy of the previous longitudinal field measurements via the lambdameter method (Bommier et al. 2005). The so-called velocity gradient ΔV is given in km s^{-1} and is the line-of-sight velocity difference between the line center and continuum formation depths.

4.2. Results

We inverted a spectropolarimetric scan of a sunspot region achieved with THEMIS on 26 August 2006 12:06 NOAA 10905 in the line Ca I 6103 Å. We used the UNNOFIT code of Bommier et al. (2007) that was improved by introducing the velocity gradient parameter. The test run showed that the inversion is faster and successfully reproduces asymmetries modeled with the velocity gradients assumption. Figure 6 displays the magnetic field solution of the UNNOFIT procedure. In Fig. 7, the field vector is drawn in terms of longitudinal (in colors) and transverse (in dashes) components. These components are expressed in the line-of-sight and plane of the sky coordinates. The magnetic field can be derived in terms of local average field strength and horizontality of the field vector. We show the additional determination of the vertical velocity gradients, whose

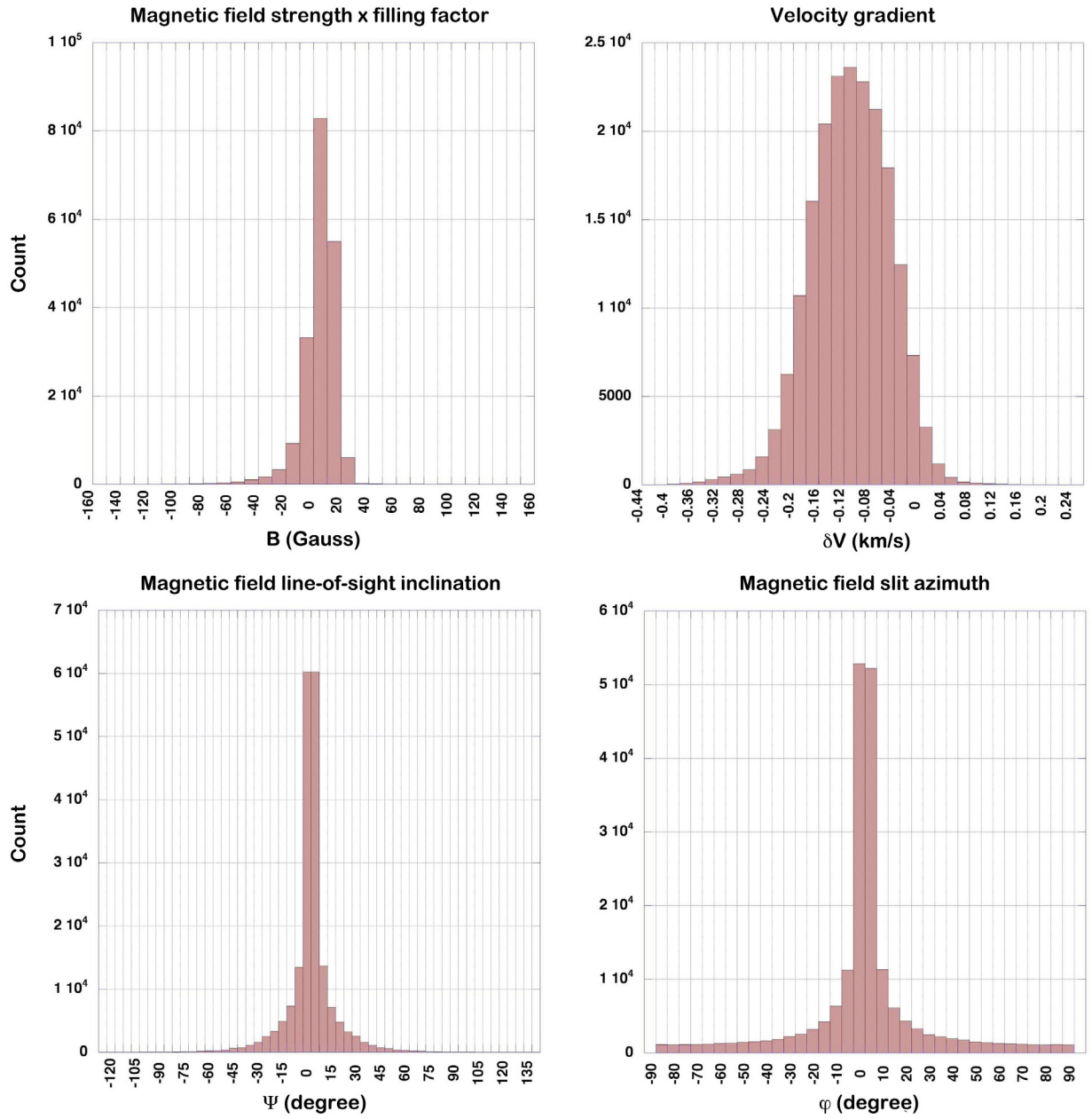

Fig. 5. Accuracy of the UNNOFIT inversion (CaI 6103 line: histograms of the differences between the UNNOFIT output values and the input ones of a series of synthetic profiles. For each ensemble of input values, a set of theoretical profiles has been computed, noised, and then inverted, leading to the output values. Histograms have been plotted for 1) the local average magnetic field strength, which is the product of the magnetic field strength by the magnetic filling factor; 2) the local velocity gradient; 3) the line of sight inclination angle; and 4) the slit's azimuth angle.

numerical value corresponds to the line-of-sight velocity difference between the line center and continuum formation depths.

5. Conclusion

We have performed UNNOFIT inversion on spectropolarimetric data obtained for Ca I 6103 Å on a sunspot. UNNOFIT is an inversion code that includes the magneto-optical and damping effects and that is based on the Marquardt algorithm applied to the Unno-Rachkovsky solution and modified to take the velocity gradient into account for the Stokes parameters emerging from a Milne-Eddington atmosphere. UNNOFIT was complemented by introducing a two-component atmosphere, with both a magnetic and a non-magnetic component. We modified the absorption coefficient entering the Unno-Rachkovsky formalism in order to derive the theoretical profiles. The theoretical profiles display asymmetries as do the observed profiles, which facilitates the inversion based on the Unno-Rachkovsky theory, and leads to the additional determination of the vertical velocity gradient. The purpose of the present work is to set the method up on exploring cases in order to model the behavior of the magnetic strength line feet (limit boundaries to reconstruct the three-dimensional shape of the coronal field).

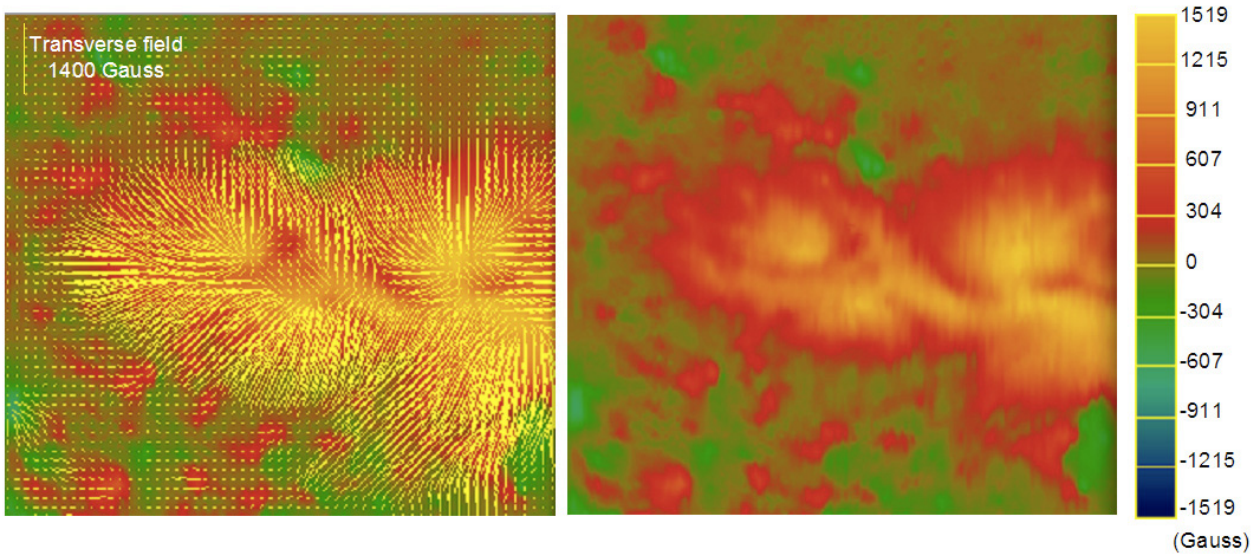

Fig. 6. UNNOFIT inversion code applied on sunspot observed the 26 August 2006 12:06 NOAA 10905 at THEMIS for ion Ca I 6103 Å. *Left*: horizontality of the field vector. *Right*: the longitudinal magnetic field component displayed in color and the transverse magnetic field in dashed lines (Gauss). The field of view is 75×71 arcsec^2.

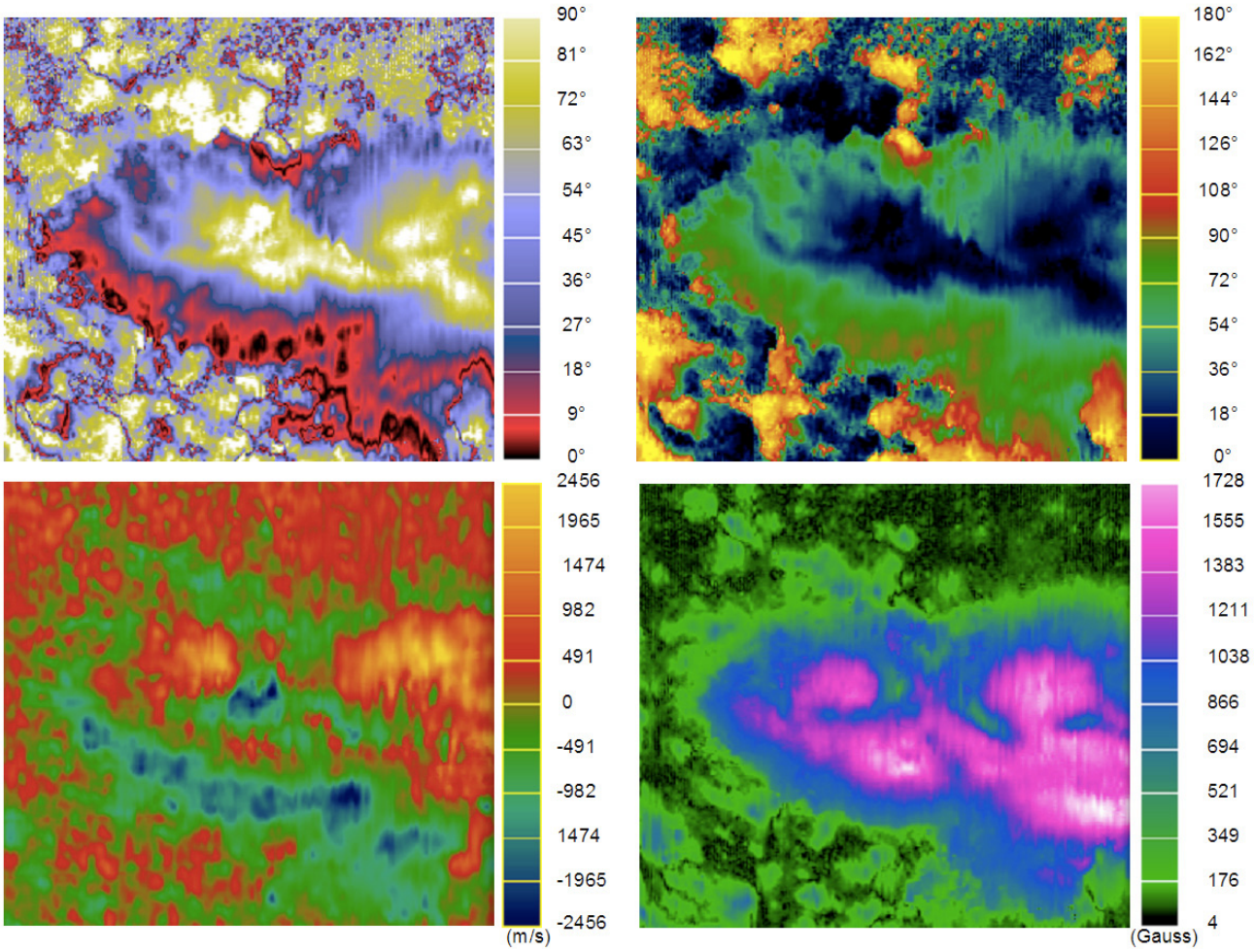

Fig. 7. UNNOFIT inversion code applied on sunspot observed the 26 August 2006 12:06 NOAA 10905 at THEMIS for ion Ca I 6103 Å. *Top left*: horizontality of the field vector. *Top right*: the azimuth of the field vector. *Bottom left*: the additional determination of the vertical velocity gradients is displayed and expressed in m s^{-1}. *Bottom right*: the magnetic field derived in terms of local average field strength (Gauss). The field of view is 75×71 arcsec^2.

Acknowledgements. In memory of our friend and colleague J. Rayrole who initiated this work. Based on observations made with the French-Italian telescope THEMIS operated by CNRS and CNR on the island of Tenerife in the Spanish Observatorio del Teide of the Instituto de Astrofísica de Canarias. Many thanks to the referee for providing constructive comments and help in improving the content of this paper.

References

Auer, L. H., & Heasley, J. N. 1978, A&A, 64, 67
Auer, L. H., Heasley, J. N., & House, L. L. 1977, Sol. Phys., 55, 44
Bommier, V., & Rayrole, J. 2002, A&A, 381, 227
Bommier, V., Rayrole, J., & Eff-Darwich, A. 2005, A&A, 435, 1125
Bommier, V., Landi Degl'Innocenti, E., Landolfi, M., & Molodij, G. 2007, A&A, 464, 323
Del Toro Iniesta, J. C., & Ruiz Cobo, B. 1996, Sol. Phys., 164, 169
Grossmann-Doerth, U. 1994, A&A, 285, 1012
Grossmann-Doerth, U., Keller, C. U., & Schussler, M. 1996, A&A, 315, 610
Harvey, J., Livingston, W., & Slaughter, C. 1972, in Line Formation in the Presence of Magnetic Fields, HAO, NCAR, Boulder, Colorado, 227
Kaisig, M., & Schröter, E. H. 1983, A&A, 117, 305
Landi Degl'Innocenti, E., & Landolfi, M. 2004, Polarization in Spectral Lines (Dordrecht: Kluwer Academ. Publ.)
Landolfi, M., & Landi Degl'Innocenti, E. 1982, Sol. Phys., 78, 355
Landolfi, M., & Landi Degl'Innocenti, E. 1996, Sol. Phys., 164, 191
Landolfi, M., Landi Degl'Innocenti, E., & Arena, P. 1984, Sol. Phys., 93, 269
Lites, B. W., & Skumanich, A. 1990, ApJ, 348, 747
Lites, B. W., Scharmer, G. B., & Skumanich, A. 1990, ApJ, 355, 329
Lopez, A. A. 2002, ApJ, 564, 379
Martinez Pillet, V., Lites, B. W., & Skumanich, A. 1997, ApJ, 474, 810
Pantellini, F. G. E., Solanki, S. K., & Stenflo, J. O. 1988, A&A, 189, 263
Rachkovsky, D. N. 1961, Izv. Crim. Astrphys. Obs., 25, 277
Ribes, E., Rees, D. E., & Fang, C. 1985, ApJ, 296, 268
Sánchez, A. J., & Lites, B. W. 1992, ApJ, 398, 359
Schroter, E. H. 1958, ZAp, 45, 68
Skumanich, A., & Lites, B. W. 1987, ApJ, 322, 473
Solanki, S. K. 1986, A&A, 168, 311
Solanki, S. W., & Pahkle, K. D. 1988, A&A, 201, 143
Stenflo, J. O., Harvey, J. W., Brault, J. W., & Solanki, S. K. 1984, A&A, 131, 333
Stepanov, V. E. 1961, Izv. Crim. Astrphys. Obs., 25, 174
Unno, W. 1956, PASJ, 8, 108
Voigt, H. H. 1956, ZAp, 40, 157